

Article

Hydration of Magnesium Carbonate in a Thermal Energy Storage Process and Its Heating Application Design [†]

Rickard Erlund * and Ron Zevenhoven

Thermal and Flow Engineering Laboratory, Åbo Akademi University, 20900 Turku, Finland; rzevenho@abo.fi

* Correspondence: rperlund@abo.fi; Tel.: +358-40-8270748

[†] This article is based on our paper, presented at ECOS 2017, 2–6 July 2017.

Received: 21 December 2017; Accepted: 8 January 2018; Published: 11 January 2018

Abstract: First ideas of applications design using magnesium (hydro) carbonates mixed with silica gel for day/night and seasonal thermal energy storage are presented. The application implies using solar (or another) heat source for heating up the thermal energy storage (dehydration) unit during daytime or summertime, of which energy can be discharged (hydration) during night-time or winter. The applications can be used in small houses or bigger buildings. Experimental data are presented, determining and analysing kinetics and operating temperatures for the applications. In this paper the focus is on the hydration part of the process, which is the more challenging part, considering conversion and kinetics. Various operating temperatures for both the reactor and the water (storage) tank are tested and the favourable temperatures are presented and discussed. Applications both using ground heat for water vapour generation and using water vapour from indoor air are presented. The thermal energy storage system with mixed nesquehonite (NQ) and silica gel (SG) can use both low (25–50%) and high (75%) relative humidity (RH) air for hydration. The hydration at 40% RH gives a thermal storage capacity of 0.32 MJ/kg while 75% RH gives a capacity of 0.68 MJ/kg.

Keywords: thermal energy storage; magnesium (hydro) carbonate; adsorption; heating systems; silica gel; geothermal heat; exhaust air heat pump

1. Introduction

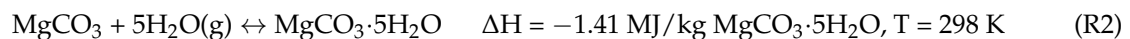
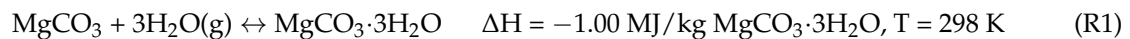
A number of renewable heat sources are not available when needed or do not meet the fluctuating demand for heating. During summer, the thermal solar heat output greatly exceeds the heating demand. Solving this problem requires seasonal storage, in the form of thermal energy storage (TES), within affordable boundaries. Moreover, in district heating systems, the seasonal storage possibility lowers the investment costs for plants in use during peak hours, and more thermal solar heating can be introduced to the system.

Using reversible chemical reactions for storage gives the highest energy density. However, this requires heat sources at 200–1000 °C, which is not applicable in most heating systems [1]. Thermal storage of heat in big water or gravel tanks has been widely tested, having a 60% efficiency (re-use of stored energy) and requiring large storage volumes underground [2]. Chemical sorption reactions require lower temperatures and are more energy dense compared to water storage tanks and require temperatures of 50–150 °C in a TES system.

Studies show that zeolite Na-Y can be used for a TES with a heat capacity 1.0 MJ/kg requiring a dehydration temperature of 140 °C. The heat capacity can be increased to 1.1 MJ/kg by combining it with 15%-wt MgSO₄, which in itself has a theoretical heat capacity of 1.74 MJ/kg [3]. However, MgSO₄ has been shown to not offer its full sorption capacity when precipitated in zeolites [3,4]. Zeolite H-Y has a 40 °C lower dehydration temperature, with a heat capacity of 0.8 MJ/kg [4]. TES with dehydration

of $\text{MgCl}_2 \cdot 6\text{H}_2\text{O}$ to $\text{MgCl}_2 \cdot 2\text{H}_2\text{O}$ gives theoretically a capacity of 2 GJ/m^3 however; using a packed bed design in the reactor with porosity of 50% reduces the capacity to 1 GJ/m^3 , and a practical test gave an efficiency as low as 0.5 GJ/m^3 [5].

Magnesite (MgCO_3) and water vapour form nesquehonite (NQ) ($\text{MgCO}_3 \cdot 3\text{H}_2\text{O}$) according to reaction (R1) or lansfordite at temperatures below $5 \text{ }^\circ\text{C}$ according to reaction (R2) [6–8]. The NQ is potentially an inexpensive resource considering it can be produced in a carbon capture and storage mineralisation (CCSM) process [8–11]. Magnesium can be extracted from serpentine mineral and carbonated in a water solution with CO_2 gas, forming nesquehonite [8]:



Moreover, the NQ can operate in lower temperatures compared to MgSO_4 , and does not require operation at a low pressure like MgCl_2 and CaCl_2 do. NQ can absorb heat by loss of crystallization water, preferably at $65 \text{ }^\circ\text{C}$, or at temperatures as low as $50 \text{ }^\circ\text{C}$, while MgSO_4 requires temperatures above $122 \text{ }^\circ\text{C}$ [4,12,13]. The lower operating temperatures increase the efficiency of solar thermal collectors (solpanels). Another advantage, in cases where the systems are placed on houses, is that NQ is considered to be a fire retardant, as it releases CO_2 and H_2O when heated [14].

Zeolites are considered to be very expensive materials for TES, while salts tested for TES are much less expensive [5]. Studies by others have shown that also silica gel (SG) can be used for this purpose instead of zeolite [4,15,16]. In this study SG is used, considering not only the lower price, but also the lower dehydrating temperature compared to zeolite which makes it more suitable to work with NQ. Dehydration of zeolite takes place at temperatures between 100 and $140 \text{ }^\circ\text{C}$ [3]. SG is fully dehydrated at $\sim 100 \text{ }^\circ\text{C}$, however, at $65 \text{ }^\circ\text{C}$ (matching NQs dehydration temperature) SG is close to fully dehydrated, which is not the case with zeolite [3,13]. This offers a better applicability with district heating operating at 50 – $110 \text{ }^\circ\text{C}$ temperatures, depending on whether it is primary or secondary district heat. Table 1 gives an overview of suitable materials and their performance.

Table 1. Operational temperatures and theoretical specific heat storage capacity of potential sorption reactions.

Reaction	Hydration Temp. ($^\circ\text{C}$)	T ($\Delta G = 0$) ($^\circ\text{C}$)	90% Dehydr. ($^\circ\text{C}$)	Dehydr. Temp. ($^\circ\text{C}$)	Specific Capacity (MJ/kg)
$\text{MgCO}_3 + 3\text{H}_2\text{O}(\text{g}) = \text{MgCO}_3 \cdot 3\text{H}_2\text{O}$	~ 20	45	61	60–65	1.0
$\text{MgCO}_3 + x\text{H}_2\text{O}(\text{l}) = \text{MgCO}_3 \cdot x\text{H}_2\text{O}$		Irrev.	Irrev.		
$\text{MgCO}_3 + 5\text{H}_2\text{O}(\text{g}) = \text{MgCO}_3 \cdot 5\text{H}_2\text{O}$	5–10	55	66	65–70	1.41
$\text{MgSO}_4 + 7\text{H}_2\text{O}(\text{g}) = \text{MgSO}_4 \cdot 7\text{H}_2\text{O}$	~ 20	145	153	122 ⁽¹⁾	1.7
$2\text{H}_2\text{O}$ ($20 \text{ }^\circ\text{C}$) = $2\text{H}_2\text{O}$ ($60 \text{ }^\circ\text{C}$)	20 ⁽²⁾	-	-	60 ⁽²⁾	0.17
Silica gel	~ 20	-	65 ⁽³⁾	100	0.62
(Silica gel dehydrated at $65 \text{ }^\circ\text{C}$)	~ 20	-	-	65	0.52
Zeolite HY [4]	~ 20	-	~ 110	110	0.8
Zeolite Na-Y (dehydrated) = Zeolite Na-Y (hydrated) [4]	~ 20	-	~ 140	140	1.0
$\text{MgCl}_2 \cdot 6\text{H}_2\text{O} = \text{MgCl}_2 \cdot 2\text{H}_2\text{O} + 4\text{H}_2\text{O}$ [5]	60	100	-	150	

⁽¹⁾ Partly dehydrates at $122 \text{ }^\circ\text{C}$ [3]. ⁽²⁾ The required operating temperatures for using water as latent heat storage with a ΔT of $40 \text{ }^\circ\text{C}$. ⁽³⁾ 85% dehydrated, matched to NQ hydration temperature.

The theoretical storage capacity of the sorption reactions in this case are 1.0 MJ/kg for nesquehonite and 0.62 MJ/kg for silica gel [6,15]. Dehydration temperatures used for NQ dehydration tests at $65 \text{ }^\circ\text{C}$ give a capacity of 0.52 MJ/kg . The dehydration part of the process is quite straightforward, with the possibility of releasing all crystallization water in 2 h, if needed. The reverse reaction, hydration of magnesite (MgCO_3), is more challenging considering conversion and kinetics. Our recent experiments with $^{50\%}/_{50\%}$ NQ (with mass equivalent to MgCO_3)-SG mixtures gave a calculated storage capacity of 0.41 MJ/kg and after 24 h hydration, being 2.4 times larger than heating up a similar mass of water from $20 \text{ }^\circ\text{C}$ to $60 \text{ }^\circ\text{C}$ [13].

countries is typically between 2.8 and 5, depending on the type and manufacturer [17]. Moreover, this system would give an extra advantage compared to air heat pumps for outside temperatures below 0 °C. In houses using solar heat, the stored heat can be used during night, or during ambient winter when temperature is e.g., below 0 °C, decreasing the required heat pump capacity. In larger houses or larger district heating systems, the usage can be centrally controlled, as more heat sources in district heating are close to the user.

2.1.1. Design of Heat Storage Process

Studies showed that a COP of 1.7–6.8 can be achieved in an open system adsorption TES, using a simple electrified humidifier [18]. Aydin et al. concluded that humidification applied to adsorption TES with low energy input requirement is challenging [19]. In order to use ground heat (at 5 °C) for evaporating the water needed for hydration, the humid air has to be pressurised to a few bar at low temperatures to reach a sufficient relative humidity (RH) for complete hydration. Shown in Figure 1, the relative humidity is increased in the evaporator containing a bubble column resulting in a RH close to 100%. The air is then heated up to the temperature in the reactor by air leaving the reactor for the evaporator in a heat exchanger. In this case, the reactor temperature is 20 °C giving a RH of 36%, which is not enough for the maximum hydration. In Figure 1 to the left, the temperature and RH of two cases (identified as 1 and 2.) are shown. The first one is the case explained above, while the second one is providing the reactor with the RH (70–75%) for maximum results obtained in earlier studies [13].

To provide 72% RH (0.011 kg H₂O/kg dry air) hydration air, the evaporator operates at 5 °C and 100% RH requires a pressure of 2 bar. Shown in Figure 1, this requires a compressor (C), which will increase the temperature to 82 °C or 50 °C when using one stage or two-stage compression, respectively. The air is cooled to 5 °C before the evaporator in a heat exchanger by the air leaving the evaporator and heated to the 82 °C or 50 °C mentioned. It then goes to the turbine, decreasing the pressure and temperature to 1 bar and 20 °C, returning the energy as work to the compressor. As a result less external electricity is required, according to the scheme to the left in Figure 1. However, this would be the case when maximum hydration is achieved, and case 1 is at the start of the hydration. Studies have shown that the concept of using ground heat for evaporating water for hydration is sufficient [5]. However, these tests were done in the Dutch climate giving a 10 °C ground heat temperature, which is considerably higher than the 5 °C (approximately 0–5 °C in southern Finland) used in this study. The higher ground temperature in the regions of central Europe (and similar climates) would decrease (or remove) the need of pressuring the evaporator. In this study, the hydration performance at different RH are tested to determine the pressures needed for operation of the evaporator, which is reported in Section 4. Further process operation opportunities will be discussed in Sections 4.2 and 4.4.

2.1.2. Charging Process

The charging process of the heat storage, dehydration of NQ and SG, is relatively simple. Shown in Figure 1 (to the right), as the reactor content heats up to 50–65 °C, crystal water is released from NQ forming MgCO₃ and absorbed water from the pores in SG. The water is cooled to the temperature of the water collector and condensed in a heat exchanger/condenser, heating up the chilled air (RH 100%) pumped from the water collector to 50–65 °C resulting in a RH of 5–10%. The air flow is minimized to avoid heat losses in the system. As mentioned earlier, the most preferable temperature for dehydration is 65 °C however, at least 50 °C is required. In Figure 2, showing results from earlier studies, the dehydration conversion was 100% and 106% at 65 °C. The result giving conversion larger than 100% is presumably caused by incomplete drying during the preparation, or lansfordite was formed in the precipitation of NQ, which was the reason why one more test was done at 65 °C. Hydration at temperatures 50–60 °C gives conversion levels of about 90% [13].

Since the temperature of 65 °C might not (always) be available, the reactor should be divided in sections. In order to store heat if only 50 °C heat is available, a different section could be used

than if 65 °C heat is available while the reaction stage of dehydrating from 90 to 100% is ongoing. Moreover, using such sections can avoid heat output problems, as the kinetics of the reaction may differ depending on the conversion grade. The sections can also be useful with day/night heat storage and seasonal storage working simultaneously. Also, different loads on the compressor during hydration could be applied by using various sections in different stages of the hydration, requiring varying RH dependent on evaporator pressure, which is discussed further in Sections 4.2 and 4.4. The relative humidity during the hydration is crucial for the performance of the system.

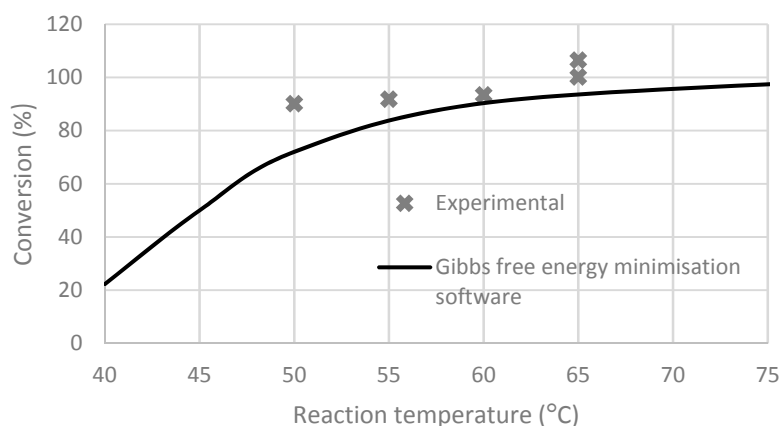


Figure 2. Dehydration conversion results after 120 min and theoretical conversion calculated using Gibbs free energy minimisation software [13].

Studies show that thermal storage of heat in certain water and gravel systems gives energy (heat) losses of 60% [2]. In the here proposed system, the reactor would have only small heat losses to the ambient, as the unused reactor section can reach ambient temperature. Stopping the airflow during hydration or dehydration stops the reactions. In this concept the air system is closed and a few percent of the air needs to contain CO₂, for NQ not to release CO₂ and form hydromagnesite (HM) (Mg₅(OH)₂(CO₃)₄·4H₂O), which would not form magnesite by dehydrating [7,8].

2.2. TES Combined with Exhaust Air Heat Pump

Our recent studies showed that the formation of HM in NQ samples is very slow at room temperature (21 °C). Samples were kept for 1 week, 2 weeks and 2 months under atmospheric conditions for comparison with the original sample. The risk of emitting 1 out of 5 CO₂ from NQ resulting in HM (not reversible) can be monitored by scanning electron microscopy (SEM) [9,20,21]. As mentioned earlier, according to Hill et al. NQ forms HM if stored under 1% of CO₂ at 25 °C, and under 0.1% of CO₂ at 10 °C although, the rate of this process seems to be unknown [7]. In Figure 3, dried NQ without aging is shown and in Figure 3a, a two months aged material stored without excess CO₂, showing no visible amounts of HM. In Figure 3b, the sample used for 20 tests is shown, and the NQ is clearly visible although, also rose-alike clusters are visible. According to other researchers, NQ crystals are needle shaped and HM crystal are shaped as irregular flakes in spherical clusters [21,22]. Moreover, the amount of HM seems not to affect the cyclability and hydration of the sample (Named Sample 1 Section 4).

Presumably, the formation of hydromagnesite occurs at high temperatures during dehydration, and hydration without excess CO₂ is possible without losing cyclability. This is why a simpler (less expensive) concept is also presented, without excess CO₂ during hydration. TES coupled with an exhaust air heat pump (EAHP) was developed, shown in Figure 4. TES using water vapour from the indoor air, of which heat is used for the EAHP and is chilled down to 4 °C, giving a suitable 60–100% RH for the hydration of NQ and SG is shown in the scheme in Figure 4. The temperature rises by 5–10 °C, depending on the available content of water vapour (giving heat when reacting with NQ

mixed with SG according to R1) per mass air heated air. This is used for preheating the inlet air, and less energy for heating inlet air is then demanded from the heating system. Basically, the water vapour source for chemisorption is excess moisture from indoor activities (shower etc.) and the outdoor air, considering that the outlet air is drier than the inlet air (due to the water vapour adsorption in the TES).

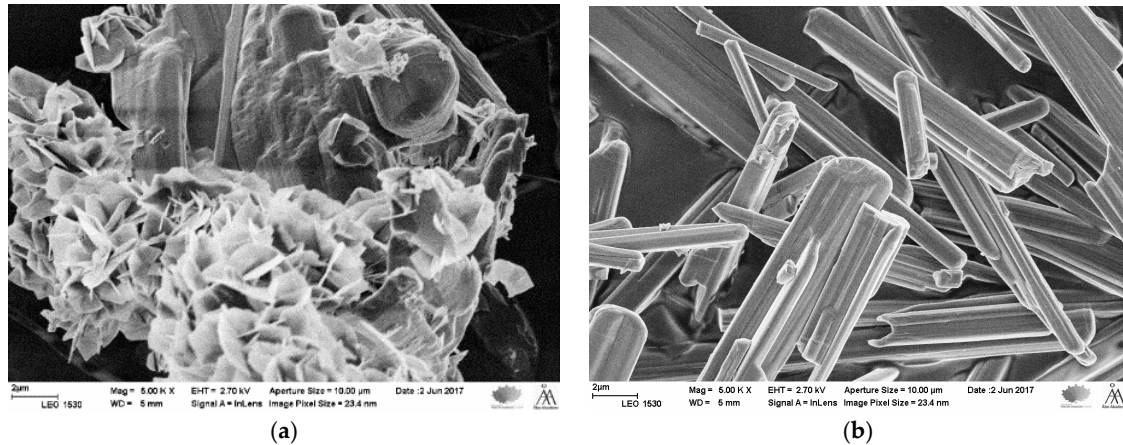


Figure 3. Left (a) NQ stored 2 month in air, Right (b) NQ twenty times dehydrated and rehydrated.

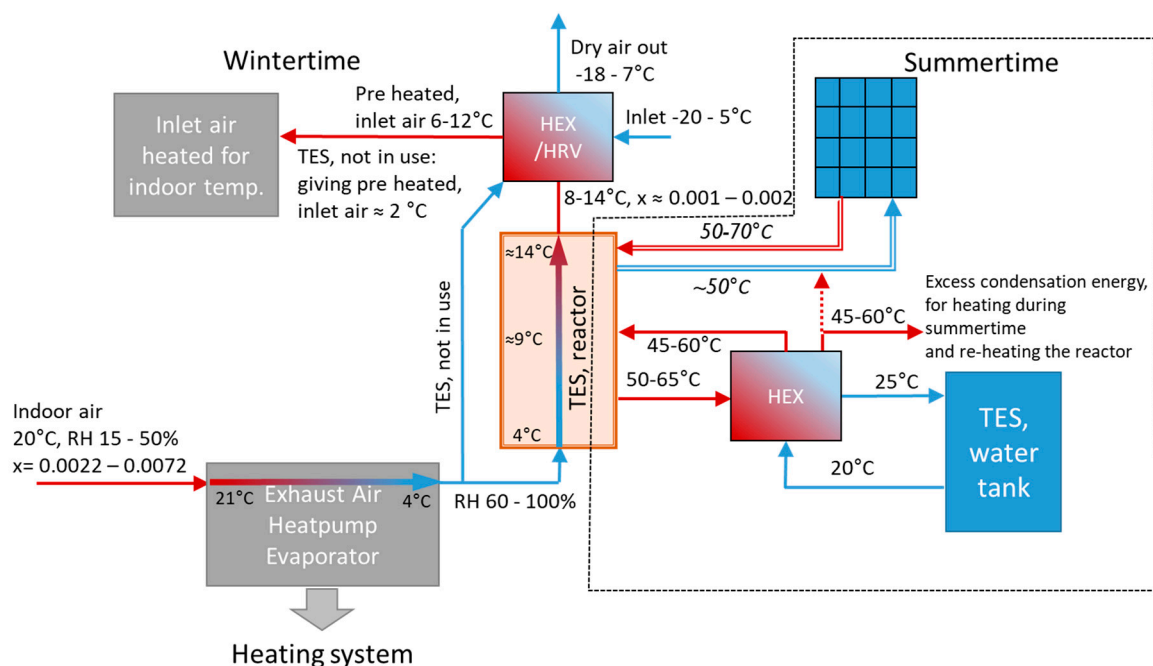


Figure 4. Scheme of the thermal energy storage reactor combined with an auxiliary heat pump.

EAHP often requires an auxiliary plant or heat source and for colder days [23]. Considering this, the heat stored during summer in a TES could be used as an assisting heat source where EAHPs are used during winter. Studies show that a modern EAHP can have a COP of 3 for producing domestic heating water and 3.4 when providing heat for floor heating [24]. During colder days, the COP of the total system could be increased using more heat, considering that the TES discharge only requires one extra fan as electricity input.

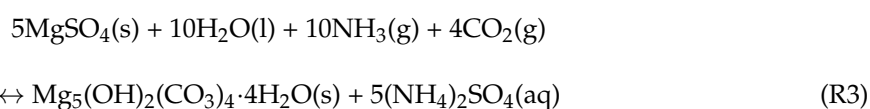
As benefits of the concept, compared to the one presented in Figure 1, no compressors and no underground water tank are required and only one more heat exchanger is needed during the

hydration. The dehydration processes for both concepts are similar although a small CO₂-bottle is required to inject an amount for 3% of CO₂ in the reaction air/gas when the dehydration season begins. During the summertime, dehydration period, the system will be closed. However, it will be limited by the operation of the EAHP. The reactor in this concept could also contain other compound with water vapour-adsorbing properties.

3. Experimental Design and Procedure

3.1. Production of Nesquehonite

As mentioned earlier, nesquehonite (NQ) is a product of a CCSM process and precipitated in a solution containing MgSO₄ into which ammonia and CO₂ are absorbed [8–11]. At temperatures above 50 °C hydromagnesite (HM) and ammonium sulphate are formed according to reaction (R3) and below 50 °C NQ and ammonium sulphate are formed [8,20,21]. Moreover, if the CO₂ vapour pressure is below 0.01 bar at lower temperatures reaction (R3) is favoured over reaction (R4) [8].



A 0.5 L solution of 0.8 mol/L MgSO₄ with CO₂ gas bubbled until reaching a pH of 4.5 was prepared. Then, 40 ml 25%-wt ammonia in water was added to increase the pH, and NQ started to precipitate at pH 9.3 and the final pH value was 9.6. The precipitate was filtered and washed to remove any unreacted MgSO₄. Dried MgSO₄ forms an impenetrable crust, which was found to decrease the hydration capacity in MgSO₄-zeolite mixtures [4]. Our earlier studies showed that several washing steps were required using this NQ preparation method, as presumably a MgSO₄ crust decreases the hydration capacity of NQ-silica Gel (SG) mixtures [13].

3.2. Preparation of Nesquehonite and Silica Gel Granule Mixture Samples

The contact between NQ and SG and between SG and the humid air is important for sufficient hydration. Three samples with the mass ratios of 5 g-1 g, 4 g-2 g and 3 g-3 g of NQ (equivalent to dehydrated NQ) and dry SG mixtures in granules of 3–6 mm were prepared. For the granulation, wet SG, powdered NQ and added 1 g water were shaken on a sieve for the size 0.5 mm. Before the hydration tests, the samples were dehydrated at 65 °C.

3.3. Hydration Experiments

In order to simulate the reactor in the process shown in Figure 1, tests with various RH were made with the NQ/SG samples. A ~20 cm high water filled bubble column was located in an isolated box, enabling regulation of the temperature of the bubble column with a heated plate or ice cubes, and to control the RH in the test. Instead of increasing the pressure in the bubble column to reach higher RH as described Section 2.1.1, according to Figure 1, the temperature of the bubble column was adjusted.

The results of this test shows the hydration efficiency at different moisture levels, which can be calculated to the pressure needed for a certain hydration level. The humid air containing 3% CO₂ is pumped from the bubble column to the reactor however. Again, the air in the reactor is pumped into the bottom of the bubble column through a porous metallic cylinder for sufficient bubble distribution. No heat exchanger shown in Figure 1 was used, as the pipes between the bubble column and the reactor were not insulated and the air flow was low (0.1 L/min), considering that the main objective for the experiments at this point was to determine the hydration performance and not (yet) the energy efficiency.

To test the kinetics and conversion of the NQ/SG mixed granules according to Figure 4 (TES combined with EAHP), the sample was placed in a cooled box at a temperature around 10 °C and the correct RH, as no additional CO₂ was supposed to be present. The same test was done at 20 °C for comparison with the test done in air with added CO₂.

4. Results

4.1. Relative Humidity Dependent Hydration

The aim of the hydration tests to determine the hydration of dehydrated NQ (MgCO₃) forming crystal water, and SG absorbing water vapour. Several tests for determining the hydration performance on, 50%-wt/50%-wt dehydrated NQ and dry silica gel (NQ+SG), dependent on RH between 25% and 85% with sample 1 were done. The best results of NQ+SG were obtained with RH 75%, varying between a mass increase of 0.25 g/g_{sample} and 0.29 g/g_{sample}, while increasing the RH to 85% did not increase the hydration. Tests at lower moisture levels with the RH of 40, 46 and 52% showed a mass increase between 0.14 g/g_{sample} and 0.19 g/g_{sample}. However, the fluctuation of the hydration performance in this range is large, considering that the best result is 35% larger than the smallest. At lower RH (25%), a mass increase of 0.093 g/g_{sample} was obtained, indicating that NQ adsorbs moisture at very low RH.

Noticeably, the mass increase of NQ+SG and SG reference samples give fairly similar results in terms of mass increase at RH 75%, while at RH 40–52% the SG seems to hydrate considerably more than the NQ+SG mixture. This suggests that NQ incorporates less water vapour than SG at RH 40–52%. The theoretical maximum for reaction R1 is 0.64 g/g_{sample} and, approximately 0.35 g/g_{sample} for water trapped in SG, if heated to 105 °C. The best result of this sample NQ+SG obtained the same mass increase as the reference SG and assuming both components hydrating equally well, gives a calculated heat storage capacity of 0.49 MJ/kg.

All of the tests shown in Figure 5 were done with the same sample of NQ+SG mixture granules and reference sample of SG. The granules and the reference SG sample have been used for twenty tests during a period of one year, with no significant change in hydration capacity or rate.

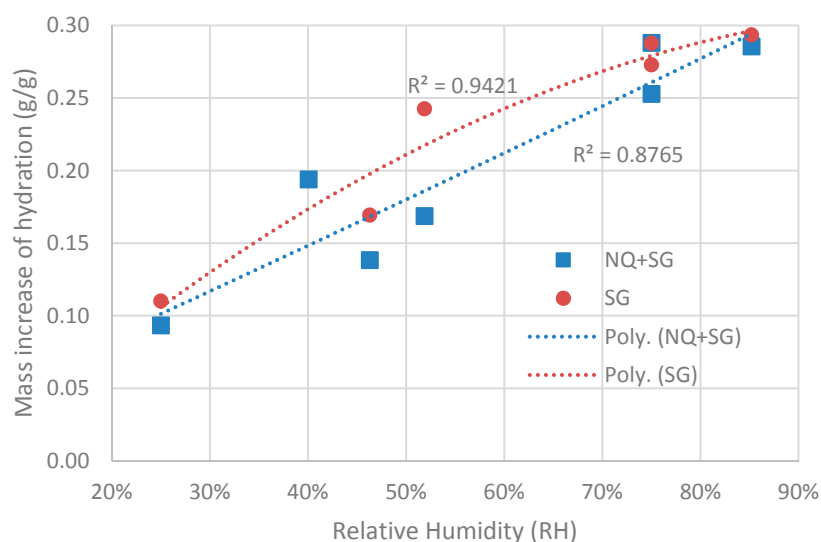


Figure 5. Mass increase of hydration versus relative humidity (RH) of 50%-wt/50%-wt silica gel and dehydrated NQ, and pure silica gel for reference. (Experiment duration 48 h).

Two test were done with sample 2 at RH of 25–30% and 75%. Shown in Figure 6, the higher RH resulted in a hydration of 0.41 g/g_{sample} giving a calculated heat storage capacity of 0.68 MJ/kg, which is near four times larger than the capacity of heat storage using the same mass of water with ΔT of

40 °C. The result is significantly better than sample 1 (0.49 MJ/kg) and results from our earlier studies (0.41 MJ/kg) [13].

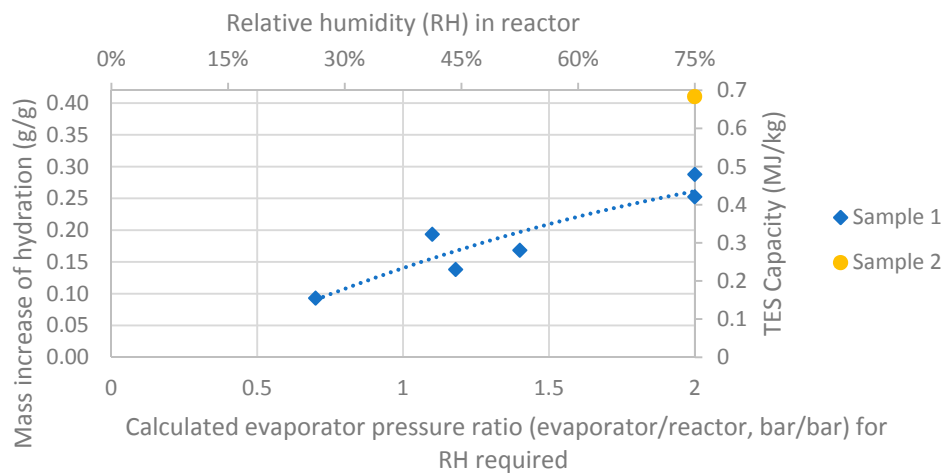


Figure 6. Mass increase of hydration and TES capacity versus relative humidity (RH) and evaporator pressure for 50%-wt/50%-wt silica gel and dehydrated NQ, and pure silica gel for reference (Experiment duration 48 h).

However, depending on the bulk density and design of the material placed in the reactor e.g., as a packed bed, the volumetric storage compared to water capacity can vary.

Shown in Figure 7, the hydration time is not significantly affected by the lower RH, considering the hydration levels reached after 18 h are close to, or similar to the final value of mass increase. However, in the test with 40% RH, a mass increase from 0.14 to 0.19 g/g_{sample} was obtained between 24 and 48 h. This indicates that the kinetics of the TES system will not be compromised while operating at lower RH, as a large fraction of the hydration is possible with at lower RH in reasonable time. In case of day/night heat storage, several days of hydration may take place, considering that cloudy or stormy days may give much lower amounts of solar heat.

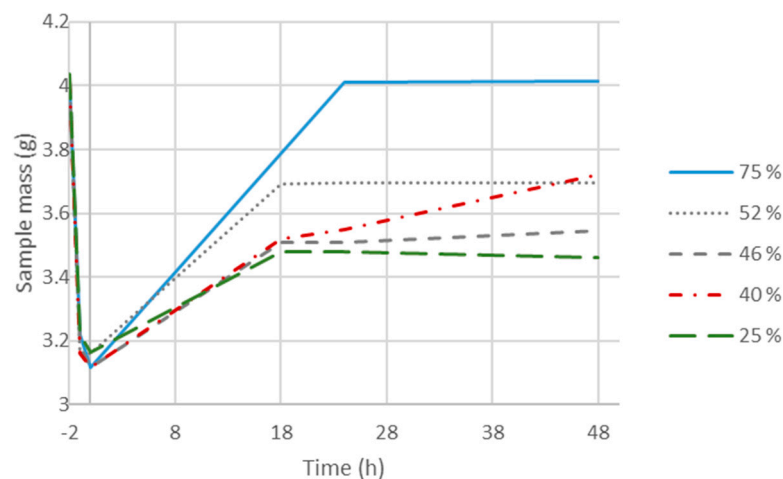


Figure 7. Mass difference on the NQ+SG granule mixture sample, during dehydration (−2 to 0 h) and hydration (0 to 48 h).

4.2. Heat Storage Efficiency and Operational Opportunities

As mentioned in Section 2.1.1, the RH of the air reaches levels up to 36% when pumped from the evaporator at 5 °C (the temperature of the ground) if no overpressure is applied. By pressuring the

evaporator according to Figure 1, a higher RH can be obtained in the reactor. The increased RH and absolute humidity (AH) of pressuring ($p_{\text{evaporator}}$) the evaporator are shown in Table 2 [25]. Dew point, hydration results and heat storage capacity, with the assumption of both component was hydrated equally are also shown in Table 2.

Table 2. Data on the relation between the humidity and pressure in the evaporator, and storage capacity and hydration results after 48 h. The humid hydration gas contains 3% CO₂.

Relative Humidity in Reactor	Hydration Mass Increase (g/g _{sample})	T _{Dewpoint} at 1 bar (°C)	P _{evaporator} for 100% RH (bar)	Absolute Humidity (g/kg)	Specific Capacity (MJ/kg)	Sample Nr.
25%	0.093	0	0.7	3.7	0.16	1
36%	-	5	1	5.3	-	
40%	0.194	7	1.1	6.3	0.32	1
46%	0.138	8	1.2	6.7	0.23	1
52%	0.169	10	1.4	7.7	0.28	1
75%	0.288	15	2	11.0	0.48	1
75%	0.253	15	2	11.0	0.42	1
75%	0.293	15	4 *	22.0	0.49	1
75–80%	0.410 **	14	2	11.0	0.68	2

* The pressure in the reactor is 2 bar. ** Reaction completed after 6 days.

The result of 0.093 g/g_{sample} mass increase with 25% RH, showing that with the evaporation temperature of 0 °C, it is possible to hydrate to approximately a third of the maximum value obtained. Requiring no overpressure and a water vapour amount similar to 70% RH at 5 °C, less use of the evaporator is needed for the first third of hydration in the reactor section operated. This indicates a high efficiency for the system. The hydration result of 0.14–0.19 g/g_{sample}, which equals between half and two thirds of the best hydration result at 40–52% RH, would require pressure between 1.1 and 1.4 bar, requiring a small amount of electricity. However, for the last part of the hydration, a pressure of 2 bar is required in the evaporator to obtain the 75% RH that gives the best hydration results, indicating that the COP of the system would be lower compared to operating at lower pressures.

A reactor design with several sections gives the opportunity to switch between phases in the reactor, for optimal operation. Moreover, this gives an opportunity to regulate the electrical efficiency (or COP) of the system coupled and regulated by smart grid systems. During high electricity demand, a lower pressure (higher COP) in the evaporator can be applied, and during relatively lower electricity demand, higher pressure (lower COP) can be applied, which preferably could be operated or integrated with smart grids.

4.3. Sample Morphology, Crystal and Efficiency

According to others, NQ are needle shaped crystals (e.g., Figure 3a) and hydromagnesite (HM) is irregular flakes that in (e.g., partly in Figure 3b), which makes it of interest to analyse the crystals' appearance using SEM pictures [21,22].

Shown in Figure 8, Sample 2 has HM flakes and some undamaged NQ, besides agglomerated or partly reacted NQ, which can be compared with re-hydrated NQ by others [21]. Sample 1 (shown in Figure 3b) seems to have more HM crystal flakes, which can be a reason for its smaller hydration capacity. Moreover, in Sample 1 the NQ needles are agglomerated in a more compact shape compared to Sample 2, which could explain the lower reactivity.

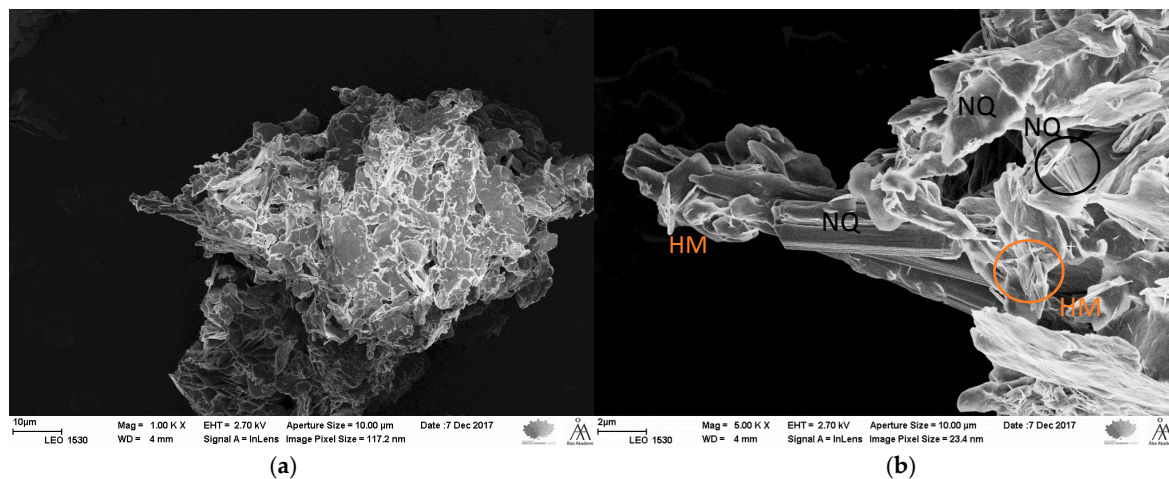


Figure 8. SEM pictures of Sample 2: (a) 1000 \times and (b) 5000 \times .

4.4. Efficiency Calculations and Improvements

The COP of the TES system (COP_{TES}) was calculated as the total heat output Q_{tot} (including the excess heat from the compressor train and the reactor heat output) divided by the electricity required for the compressor according to Equation (1).

$$COP_{TES} = \frac{Q_{tot}}{\frac{1}{\eta_{electric}} \cdot (W_{comp} - W_{turb})} \quad (1)$$

Other losses (e.g., heat exchange) in the system were neglected, as minimising the efficiency penalty of compressing gas for water vapour generation is the major challenge. Overall compressor and turbine efficiency of 0.88 were chosen for the calculations although these efficiencies depend on several factors (flow coefficients and device quality to name a few) [26].

The work required for the generation of water vapour, according to Figure 1, would approximately give a COP_{TES} of 2–4 depending on whether a pressure of 1.41 or 2 bar is used in the evaporator and the reactor, as shown in Table 3. However, the COP_{TES} can be improved by two different methods. Firstly, increasing the total pressure in the system, giving a larger absolute humidity, decreases the amount (mass) of compressed gas per mass water vapour [25]. Increasing the reactor pressure to 2 bar gave a slightly better hydration test result of 0.293 g/ g_{sample} mass increase, giving a storage capacity of 0.49 MJ/kg, as shown in Table 2. Figure 9 shows that at a higher pressure both the dehydration and hydration reactions will take place at slightly higher temperature, according to Gibbs free energy calculations. Secondly, coupling two circuits in series, decreasing the temperature difference in each individual circuit, leads to decreased requirements for water vapour generation at lower temperatures according to the results shown in Table 3. A smaller temperature difference between the evaporator and the reactor requires a lower pressure in the evaporator for a certain RH in the reactor and requires less compressor work.

In Figure 10, an improved concept of the system with two circuits is shown. Assuming similar chemical reaction behaviour of the material at 15 °C and 25 °C, two circuits in series would improve the COP when maximum heat storage capacity is achieved (when a higher RH is used in the reactor). As shown in Table 3, this gives a COP_{TES} of about 7 in the first circuit with 5 °C in the bubble column (located underground) and 15 °C in the reactor, or a COP_{TES} as high as about 11 in the second circuit with 15 °C in the bubble column and 25 °C in the reactor. It gives a COP_{TES} average of 4.5, when the reactor pressure is 3 bar and evaporator 4.32 bar. Shown in Figure 11, approaching 20 °C temperature in the similar case, the COP would be 5.6. A 5 °C higher end temperature would decrease the temperature rise to be realised by the heat pump. However, this COP_{TES} value is only valid when the reaction is

reaching full hydration and maximum heat storage is used, being larger when a lower RH is used. The single circuit system had a COP_{TES} of 4.6, with a reactor operated at 3 bar, while approaching 20 °C, and with lower RH (55%), giving a storage capacity of 0.32MJ/kg, the COP_{TES} is 6.4.

Table 3. The COP_{TES} depending on pressure and temperature in both the evaporator and reactor, number of circuits and compressor/turbine efficiency. One system circuit is calculated according to process scheme in Figure 1 and two circuit system calculated according to process scheme in Figure 10.

T _{evaporator} (°C)	P _{evaporator} (bar)	T _{reactor} (°C)	P _{reactor} (bar)	Relative Humidity, Reactor (%)	Storage Capacity (MJ/kg)	COP _{TES}	System Circuits
5	2	20	1	75%	0.48	2.2	1
5	1.41	20	1	55%	0.32	2.8	1
5	1	20	1	36%	0.22	No Comp.	1
5	1.41	15	1	75%	0.48 ⁽¹⁾	3.0	2
15	1.41	25	1	75%	0.48 ⁽¹⁾	4.3	2
5	4	20	2	75%	0.49	3.3	1
5	2.82	20	2	55%	0.32	4.6	1
5	4.32	20	3	55%	0.32	6.4	1
5	4.32	15	3	75%	0.49 ⁽³⁾	7.0 (4.5) ⁽²⁾	2
15	4.32	25	3	75%	0.49 ⁽³⁾	11 (4.5) ⁽²⁾	2
5	6	20	3	75%	0.49 ⁽³⁾	4.5	1

⁽¹⁾ Assuming that storage capacity is similar to test done at 20 °C. ⁽²⁾ Total COP_{TES} of a two-step process. ⁽³⁾ Assuming the capacity is similar to reaction at 2 bar.

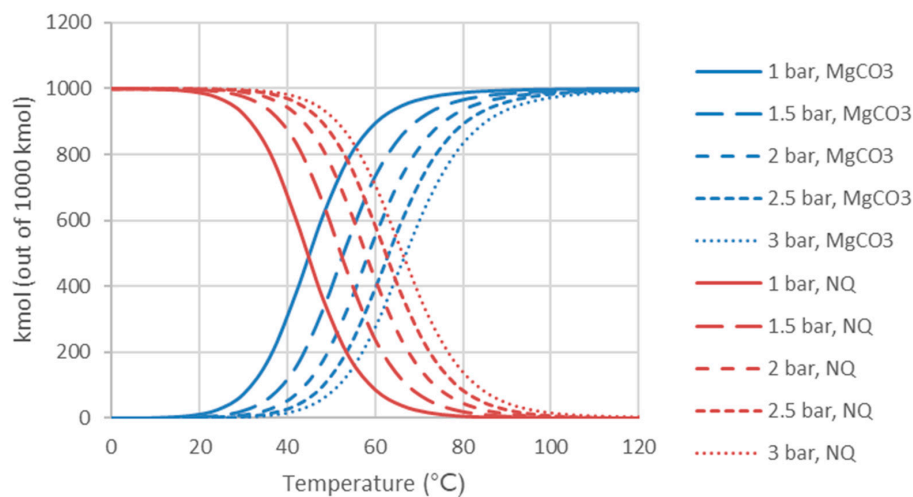


Figure 9. Gibbs energy minimization of reaction $MgCO_3 + 3H_2O = MgCO_3 \cdot 3H_2O$ for various pressures.

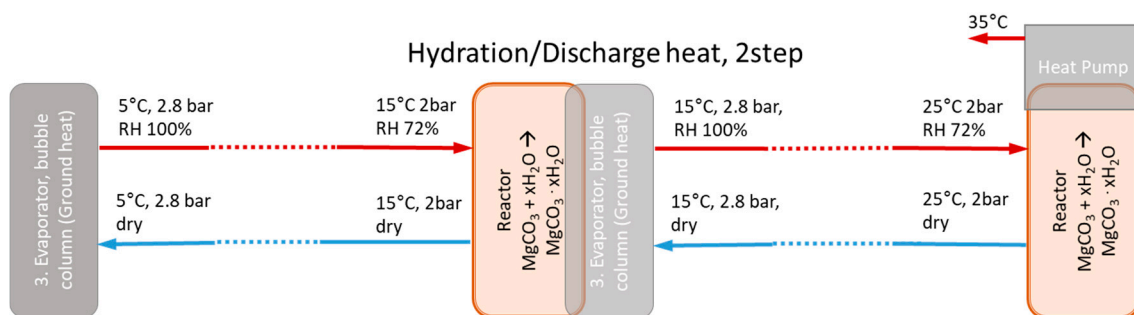


Figure 10. Scheme of the hydration step with two circuits in the thermal energy storage process. The dotted lines stands for the compressor, turbine and heat exchanger similar system shown in Figure 1. The reactor is at 15 °C. Evaporator 2 is integrated with Reactor 1 to minimise the temperature difference.

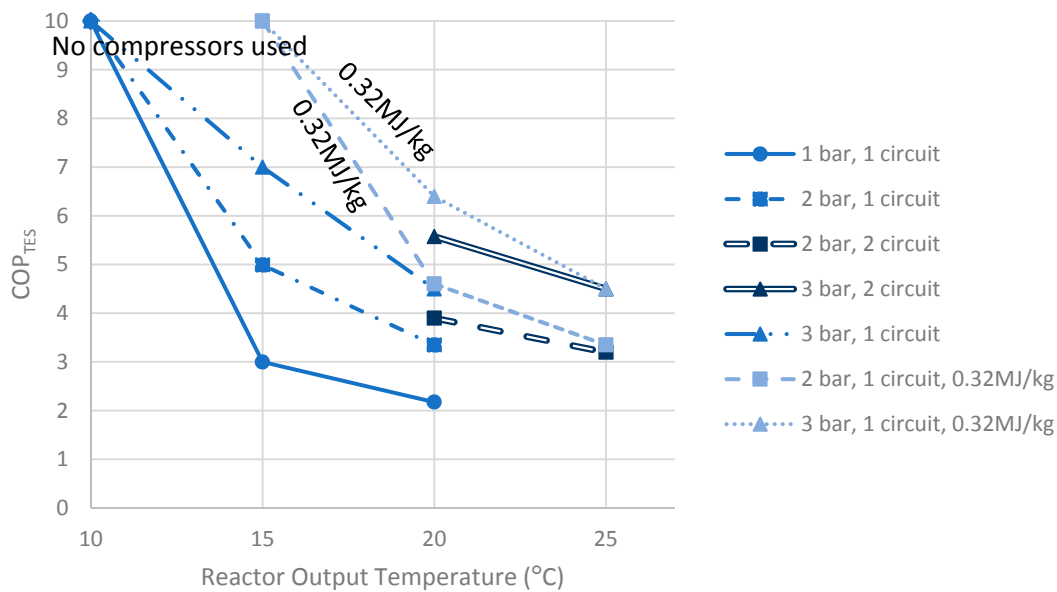


Figure 11. COP calculations with relative humidity 75% in the reactor and 5°C in the evaporator, various reactor temperature. The COP_{TES} values of 10 are approximate as no compressors are used, and only fans will be used. Compressor/turbine efficiency: $\eta = 0.88$.

This gives an interesting optimisation challenge, depending on whether using two circuits or using less compression (giving only 0.32 MJ/kg and improved COP_{TES}).

4.5. Output of Reactor Coupled with Exhaust Air Heat Pump (EAHP)

Two tests were done without CO_2 , in the hydration phase, at operation temperature 8–11 °C according to the process scheme in Figure 4, and at 20 °C for comparison with the test done with 3%-vol CO_2 . Shown in Table 4, the mass increase at operation temperature is 0.214 g/g_{sample}, giving a calculated heat storage capacity of 0.36 MJ/kg. However, at 20 °C and 95% RH a mass increase of 0.422 g/g_{sample} was achieved, giving a calculated heat storage capacity of 0.70 MJ/kg, which is slightly larger than 0.41 g/g_{sample} at 75% and 3%-vol CO_2 shown in Figure 6. This suggests that the CO_2 amount and RH above 75% does not affect the hydration significantly. However, the lower operation temperature of 8–11 °C, with about 2.5 times lower absolute humidity, results in half hydration conversion. The reaction kinetics seems not be affected by the lower reaction temperature in earlier studies (compared to 20 °C), releasing about 70% of the energy storage capacity during 24 h.

Table 4. Data on test without CO_2 using sample 2, according to the process scheme in Figure 4.

Relative Humidity in Reactor	Hydration Mass Increase (g/g _{sample})	Temperature (°C)	Reactions Time until Stagnation	Absolute Humidity (g/kg)	Specific Capacity (MJ/kg)	Sample Nr.
65–75%	0.214	8–11	4 days	0.053	0.36	2
95%	0.422	20	2 weeks	0.14	0.70	2

The heat effect of the TES reactor giving a temperature increase depending on the water vapour available are shown in Figure 12. The heat output of the TES would be 22–32% of the EAHP, depending on the RH of the indoor air. In the calculations, the RH of the output air from the reactor is 25% at the temperature of 4 °C (output temperature from EAHP) + ΔT , temperature increase (in the reactor).

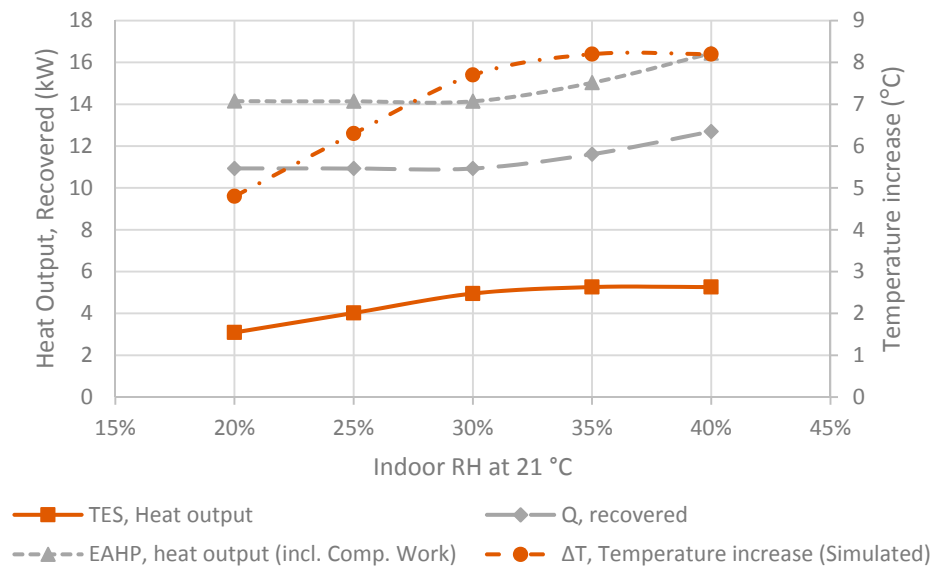


Figure 12. The heat recovered using EAHP and with compressor work added, giving EAHP total heat output in grey. The COP of the EAHP used for the calculations is 3.4, which is an experimental value presented by others [24]. Shown in orange, is the TES heat output and the temperature increase in the reactor showed.

4.6. Silica Gel/Nesquehonite Mass Ratio

Considering that NQ has a better heat storage capacity (per volume) and would be a less expensive resource than SG, testing hydration performance on mixtures with higher amounts NQ per SG was done aiming at lower material costs. Figure 13 shows that the double amount of NQ per SG (4 g per 2 g) will decrease the hydration to a 0.105 g/g_{sample} mass increase, which is not sufficient. The result is very close to the hydration of 0.096 g/g_{sample} with the mass ratio of 5 NQ per SG (5 g per 1 g). This indicates that if SG contact with air is compromised, the mass increase of hydration is close to 0.1 g/g, and the optimal mixture is between 1 and 2 NQ per SG (1–2 g/g).

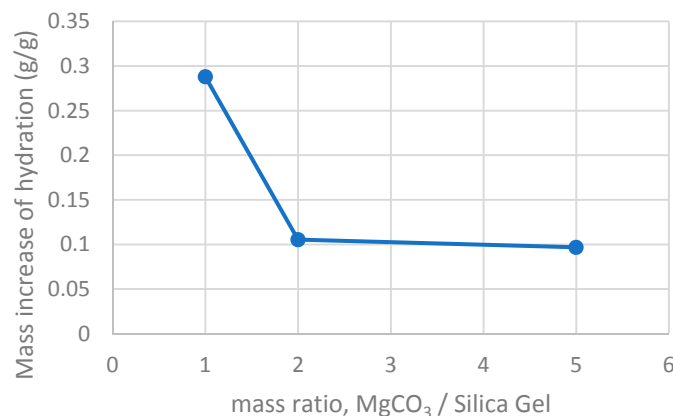


Figure 13. The mass ratio of dehydrated NQ in form of MgCO₃ per SG in granules 3–6 mm versus hydration in form of mass increase after the reaction was stabilised at 24 h.

5. Conclusions

A thermal energy storage (TES) system using mixed nesquehonite (NQ) and silica gel (SG) can use both low (25–50%) and high (75%) relative humidity (RH) air for hydration. The hydration at 40% RH gives a thermal storage capacity of 0.32 MJ/kg and at 75% RH gives a capacity of 0.68 MJ/kg.

Therefore, the system can initially work at lower RH, which is more energy efficient, and later at higher RH to complete the hydration.

Sufficient levels of coefficient of performance for the thermal energy storage system can be achieved with:

- increased absolute humidity by operating the hydration reactor at slightly elevated pressure.
- using a two (instead of one) circuit system decreasing the temperature difference in the system, decreasing the pressure difference between the evaporator and reactor.
- sufficiently high compressor and turbine efficiency.
- exhaust air heat pump (EAHP) chilled outlet air, with high RH, eliminating the compressor requirement.

The kinetics of the TES system are not compromised when operating at lower RH, as a large fraction of the hydration is possible with at lower RH in reasonable time. When combining the TES reactor with EAHP, the additional heat output of the TES is 22–32% of the EAHP. The optimal weight ratio between dehydrated NQ and SG is between 1 and 2 MgCO₃/SG.

Acknowledgments: The authors want to acknowledge Fortum Foundation, K.V. Lindholms Stiftelse and Erkki Paasikivi Foundation, for financial support for this work.

Author Contributions: Rickard Erlund and Ron Zevenhoven together developed the concept of TES using hydrated magnesite into an experimental assessment supported by model calculations. Rickard Erlund carried out the experimental work, produced the first designs of the process schemes presented and wrote the first draft of the paper.

Conflicts of Interest: The authors declare no conflict of interest.

Abbreviations

AH	Absolute humidity
COP	Coefficient of performance
COP _{TES}	Coefficient of performance for the TES system
EAHP	Exhaust air heat pump
HM	Hydromagnesite
NQ	Nesquehonite
P _{evaporator}	Pressure in the evaporator/bubble column
P _{reactor}	Pressure in the adsorption reactor
Q _{tot}	Total heat effect of the TES system, including heat from the reactor and waste heat from compressor work
RH	Relative humidity
SEM	Scanning electron microscope
SG	Silica gel
TES	Thermal energy storage
T _{evaporator}	Temperature in the evaporator/bubble column
T _{reactor}	Temperature in the adsorption reactor

References

1. Edem N'Tsoukpoe, K.; Liu, H.; Le Pierrès, N.; Luo, L. A review on long-term sorption solar energy storage. *Renew. Sustain. Energy Rev.* **2009**, *13*, 2385–2396. [[CrossRef](#)]
2. Bauer, D.; Marx, R.; Nußbicker-Lux, J.; Ochs, F.; Heidemann, W.; Müller-Steinhagen, H. German central solar heating plants with seasonal heat storage. *Sol. Energy* **2010**, *84*, 612–623. [[CrossRef](#)]
3. Whiting, G.; Grondin, D.M.; Bennici, S.; Auroux, A. Heats of water sorption studies on zeolite–MgSO₄ composites as potential thermochemical heat storage materials. *Sol. Energy Mater. Sol. Cells* **2013**, *112*, 112–119. [[CrossRef](#)]
4. Hongois, S.; Kuznik, F.; Stevens, P.; Roux, J.-J. Development and characterization of a new MgSO₄-zeolite composite for long-term thermal energy storage. *Sol. Energy Mater. Sol. Cells* **2011**, *95*, 1831–1837. [[CrossRef](#)]

5. Zondag, H.; Kikkert, B.; Smeding, S.; de Boer, R.; Bakker, M. Prototype thermochemical heat storage with open reactor system. *Appl. Energy* **2013**, *109*, 360–365. [CrossRef]
6. *HSC Chemistry*, version 8.1.1; Reaction Equations; Outotec: Pori, Finland, 2014.
7. Hill, R.J.; Canterford, J.H.; Moyle, F.J. New data for lansfordite. *Miner. Soc.* **1982**, *46*, 453–457. [CrossRef]
8. Zevenhoven, R.; Slotte, M.; Åbacka, J.; Highfield, J. A comparison of CO₂ mineral carbonation processes involving a dry or wet carbonation step. *Energy* **2016**, *177*, 604–611. [CrossRef]
9. Zevenhoven, R.; Slotte, M.; Koivisto, E.; Erlund, R. Serpentine carbonation process routs using ammonium sulphate and integration in industry. *Energy Technol.* **2017**, *5*, 945–954. [CrossRef]
10. Koivisto, E.; Erlund, R.; Zevenhoven, R. Extraction of magnesium from four Finnish magnesium silicate rocks for CO₂ mineralisation—Part 1: Thermal solid/solid extraction. *Hydrometallurgy* **2016**, *166*, 222–228. [CrossRef]
11. Erlund, R.; Koivisto, E.; Zevenhoven, R. Extraction of magnesium from four Finnish magnesium silicate rocks for CO₂ mineralisation—Part 2: Aqueous solution extraction. *Hydrometallurgy* **2016**, *166*, 229–236. [CrossRef]
12. Morgan, B.; Wilson, S.; Madsen, I.; Gozukara, J. Increased thermal stability of nesquehonite (MgCO₃·H₂O) in the presence of humidity and CO₂: Implications for low-temperature CO₂ storage. *Int. J. Greenh. Gas Control* **2015**, *39*, 366–376. [CrossRef]
13. Erlund, R.; Zevenhoven, R. Thermal storage of (solar) energy by sorption of water in magnesium (hydro) carbonates. *Int. J. Thermodyn.* **2017**, *20*, 102–109. [CrossRef]
14. Hollingbery, L.A.; Hull, T.R. The fire retardant behaviour of huntite and hydromagnesite—A review. *Polym. Degrad. Stabil.* **2010**, *95*, 2213–2225. [CrossRef]
15. Tahat, M.A. Heat-pump/energy-store using silica gel and water as a working pair. *Appl. Energy* **2001**, *69*, 19–27. [CrossRef]
16. Lim, K.; Che, J.; Lee, J. Experimental study on adsorption characteristics of a water and silica-gel based thermal energy storage (TES) system. *Appl. Therm. Eng.* **2017**, *110*, 80–88. [CrossRef]
17. Statens Energimyndigheten, Sweden. Available online: <http://www.energimyndigheten.se/tester/tester-a-o/bergvarmepumpar/bergvarmepumpar/> (accessed on 5 December 2017). (In Swedish)
18. Johannes, K.; Kuznik, F.; Hubert, J.-L.; Durier, F.; Obrecht, C. Design and characterisation of a high powered energy dense zeolite thermal energy storage system for buildings. *Appl. Energy* **2015**, *159*, 80–86. [CrossRef]
19. Aydin, D.; Casey, S.P.; Riffat, S. The latest advancements on thermochemical heat storage systems. *Renew. Sustain. Energy Rev.* **2015**, *41*, 356–367. [CrossRef]
20. Jauffret, G.; Morrison, J.; Glasser, F.P. On the thermal decomposition of nesquehonite. *J. Therm. Anal. Calorim.* **2015**, *122*, 601–609. [CrossRef]
21. Morrison, J.; Jauffret, G.; Galvez-Martos, J.K.; Glasser, F.P. Magnesium-based cements for CO₂ capture and utilization. *Cem. Concr. Res.* **2016**, *85*, 183–191. [CrossRef]
22. Teir, T.; Kuusik, R.; Fogelholm, C.-J.; Zevenhoven, R. Production of magnesium carbonates from serpentinite for long-term storage of CO₂. *Int. J. Miner. Process.* **2007**, *85*, 1–15. [CrossRef]
23. Fracastoro, G.V.; Serraino, M. Energy analyses of buildings equipped with exhaust air heat pumps (EAHP). *Energy Build.* **2010**, *42*, 1283–1289. [CrossRef]
24. Mikola, A.; Kõiv, T.-A. The Efficiency Analysis of the Exhaust Air Heat Pump System. *Engineering* **2014**, *6*, 1037–1045. [CrossRef]
25. Ren, H.-S. Construction of a generalized psychrometric chart for different pressures. *Int. J. Mech. Eng. Educ.* **2004**, *32*, 212–222. [CrossRef]
26. How to Estimate Compressor Efficiency? Available online: <http://www.jmcampbell.com/tip-of-the-month/2015/07/how-to-estimate-compressor-efficiency/> (accessed on 5 December 2017).

